



OPEN

Novel gene-specific Bayesian Gaussian mixture model to predict the missense variants pathogenicity of Sanfilippo syndrome

Eman E. A. Mohammed^{1,5}, Alaaeldin G. Fayez^{2,5}, Nabil M. Abdelfattah³ & Ekram Fateen⁴

MPS III is an autosomal recessive lysosomal storage disease caused mainly by missense variants in the *NAGLU*, *GNS*, *HGSNAT*, and *SGSH* genes. The pathogenicity interpretation of missense variants is still challenging. We aimed to develop unsupervised clustering-based pathogenicity predictor scores using extracted features from eight in silico predictors to predict the impact of novel missense variants of Sanfilippo syndrome. The model was trained on a dataset consisting of 415 uncertain significant (VUS) missense *NAGLU* variants. Performance The SanfilippoPred tool was evaluated by validation and test datasets consisting of 197-labelled *NAGLU* missense variants, and its performance was compared versus individual pathogenicity predictors using receiver operating characteristic (ROC) analysis. Moreover, we tested the SanfilippoPred tool using extra-labelled 427 missense variants to assess its specificity and sensitivity threshold. Application of the trained machine learning (ML) model on the test dataset of labelled *NAGLU* missense variants showed that SanfilippoPred has an accuracy of 0.93 (0.86–0.97 at CI 95%), sensitivity of 0.93, and specificity of 0.92. The comparative performance of the SanfilippoPred showed better performance (AUC = 0.908) than the individual predictors SIFT (AUC = 0.756), Polyphen-2 (AUC = 0.788), CADD (AUC = 0.568), REVEL (AUC = 0.548), MetaLR (AUC = 0.751), and AlphMissense (AUC = 0.885). Using high-confidence labelled *NAGLU* variants, showed that SanfilippoPred has an 85.7% sensitivity threshold. The poor correlation between the Sanfilippo syndrome phenotype and genotype represents a demand for a new tool to classify its missense variants. This study provides a significant tool for preventing the misinterpretation of missense variants of the Sanfilippo syndrome-relevant genes. Finally, it seems that ML-based pathogenicity predictors and Sanfilippo syndrome-specific prediction tools could be feasible and efficient pathogenicity predictors in the future.

Keywords Machine-learning model, Sanfilippo syndrome, Missense variants, Pathogenicity prediction

Sanfilippo syndrome is named after Dr. Sylvester Sanfilippo, who discovered the cause of this disease in 1963. This disorder is due to the absence of specific lysosomal enzymes essential for breaking down glycosaminoglycans (GAGs), called heparan sulfate. Sanfilippo syndrome, also known as Mucopolysaccharidoses III (MPS III), is an autosomal recessive metabolic disorder caused by variants in genes responsible for the degradation of GAGs, heparan sulfate (HS), located in the extracellular membrane. The lysosomal accumulation of undegraded heparan sulfate leads to cellular dysfunction and pathology in several organs, with severe central nervous system degeneration resulting in dementia and behavioral abnormalities as the main clinical characteristics of MPS III¹. MPS III has four different subtypes designed as MPS III type A (MPS IIIA), MPS III type B (MPS IIIB), MPS III type C (MPS IIIC), and MPS III type D (MPS IIID), caused by the deficiency of one of the four lysosomal specific

¹Medical Molecular Genetics Department, Human Genetics and Genome Research Institute, National Research Centre, Giza, Egypt. ²Molecular Genetics and Enzymology Department, Human Genetics and Genome Research Institute, National Research Centre, Giza, Egypt. ³Nasser's Institute for Research and Treatment, Cairo, Egypt. ⁴Biochemical Genetics Department, Human Genetics and Genome Research Institute, National Research Centre, Giza, Egypt. ⁵These authors contributed equally: Eman E. A. Mohammed and Alaaeldin G. Fayez. ✉email: em.mohammed99@gmail.com

enzymes, heparan N-sulfatase (sulfamidase) (SGSH), alpha-N-acetylglucosaminidase (NAGLU), acetyl CoA-alpha-glucosaminidase N-acetyltransferase (HGSNAT) and N-acetylglucosamine-6-sulfatase (GNS), respectively. All subtypes of MPS III have similar clinical phenotypes and are common in the elevation of urinary heparan sulphate level².

MPS IIIB is caused by over 170 variants in the N-acetyl- alpha-D-glucosaminidase (*NAGLU*) gene, an 8.5 kb, consists of 6 exons, and is localised on chromosome 17q21. The *NAGLU* gene encodes the alpha-N-acetylglucosaminidase enzyme of 743 amino acids, with a 20–23-aa signal peptide immediately preceding the amino terminus of the enzyme and with six potential N-glycosylation sites, which catalyses the removal of the N-acetylglucosamine residues from the non-reducing terminal of heparan sulphate by lysosomal degradation³. Pathogenic *NAGLU* variants reduce the activity of this enzyme and result in lysosomal accumulation of both non-degraded and partially degraded heparan sulfate⁴. A crystalline *NAGLU* enzyme is composed of three domains (I, II, and III). Amino acids 24–126 form a small alpha/beta domain in Domain I. Domain II contains the catalytic residues, amino acids 127–467 form an (alpha/beta)8 domain. Amino acids 468–743 form an alpha-helical domain in Domain III, the active site is located between Domains II and III⁵. MPS IIIB patients are diagnosed by quantitative measurement of GAGs and two-dimensional electrophoresis of urinary GAGs⁶. The enzyme activity, alpha-N-acetylglucosaminidase (*NAGLU*) (MPS IIIB; EC 3.2.1.50) was assayed in the plasma using fluorogenic substrates⁷. The normal range of *NAGLU* activity is 10–45 µmol/l/h and for the normal cases of MPS III, the electrophoretic separation of urinary GAGs should not show heparan (H) or heparan sulfate (HS) spots.

Interpreting the effect of missense VUS variants is challenging, especially since functional study of the pathogenicity of large numbers of variants is costly and time-consuming. Consequently, many algorithms were developed to accurately predict the deleteriousness of VUS variants and improve clinical diagnosis, patient management, and personalised treatment. Peterson et al.⁸ pointed out that computational tools for variant impact prediction rely on data-derived expert knowledge or data-driven machine-learning algorithms⁸.

While the current computational tools provide inconsistent variant interpretation with each other^{9,10}, these tools neglect the gene function nature and distinct disease pathogenicity modes, disease-specific tools are in high demand now. It is well known that the complementary approach of individual computational tools has the best variant interpretation power deriving from multiple variant features and prediction algorithms.

Currently, genome-wide prediction tools have low specificity; Zhang et al.¹¹ pointed out that classifying variants as pathogenic or not, without reference to a specific disease or mechanism, may not perform as well as those that separate gene-disease relations¹¹. Moreover, Ruklisa et al.¹² showed that considering gene-disease relevance in a classification computational model improves variant interpretation¹². In addition, Richards et al.¹³ noted that genome-wide prediction tools gave over a handful for limiting false-positive assertions (type I error) and providing over-prediction of disease-causing variants¹³.

This study aims to construct a model capable of classifying pathogenic and benign *NAGLU* missense variants using unsupervised clustering. To overcome the drawbacks of genome-wide prediction tools, we combined several computational scores that consider gene-disease relations by taking missense variants, which are common in MPS III. Moreover, we tested this model on the four subtypes of MPS III relevant genes. Finally, we constructed the Excel-based “SanfilippoPred” tool that combines the four genes associated with MPS III. “SanfilippoPred” demonstrated better accuracy than the individual genome-wide tools to distinguish between the pathogenic variants and the benign variants in MPS III-relevant genes.

Results

Data on 612 variants of the *NAGLU* gene were included in the analysis. Out of 612 variants, 197 variants were labelled, of which 96 variants (48.7%) were likely pathogenic or pathogenic and 101 variants were benign or likely benign (51.3%). Genome-wide variant pathogenicity predictors (features) included Grantham's distance, Sneath's score, SIFT, PolyPhen-2, CADD, REVEL, MetaLR, and the MutationAssessor. The statistical summary of the 612 variant scores presented in Table 1.

The posterior means, 50th percentiles, and 95% credible intervals for each variable in cluster centroids of the full model (including all the variables) and the parsimonious model for 415 VUS (unlabeled) *NAGLU* missense variants are presented in Table 2. For the full model, 238 out of 415 VUS variants (57.3%) were classified as pathogenic, and 177 out of 415 (42.7%) were classified as benign variants. It is noted that the sampler converged to values consistent with each score value denoting a benign or pathogenic variant. The full model

| | Features* | | | | | | | |
|--------|-----------|--------|-------|------------|--------|-------|--------|------------------|
| | Grantham | Sneath | SIFT | PolyPhen-2 | CADD | REVEL | MetaLR | MutationAssessor |
| Min | 5.000 | 5.000 | 0.000 | 0.000 | 0.000 | 0.124 | 0.000 | 0.000 |
| Max | 215.000 | 43.000 | 1.000 | 1.000 | 32.000 | 0.995 | 0.997 | 0.951 |
| Range | 210.000 | 38.000 | 1.000 | 1.000 | 32.000 | 0.871 | 0.997 | 0.951 |
| Median | 64.000 | 23.000 | 0.040 | 0.595 | 23.000 | 0.576 | 0.915 | 0.671 |
| Mean | 76.761 | 23.279 | 0.188 | 0.526 | 19.466 | 0.590 | 0.882 | 0.610 |
| SD | 44.707 | 9.186 | 0.269 | 0.420 | 8.077 | 0.263 | 0.112 | 0.291 |

Table 1. Descriptive statistics for the 612 variants according to their calculated features. *SIFT, sorting intolerant from tolerant; CADD, combined annotation dependent depletion, PolyPhen, polymorphism phenotyping; REVEL, rare exome variant ensemble learner.

| | Benign | | | | Pathogenic | | | |
|---------------------------------|--------------------|-------|-------|-------|--------------------|-------|-------|-------|
| | Mean (\pm SD) | 2.50% | 50.0% | 97.5% | Mean (\pm SD) | 2.50% | 50.0% | 97.5% |
| Full model | | | | | | | | |
| Cluster weights (ω_k): | 0.43 (\pm 0.03) | 0.39 | 0.43 | 0.49 | 0.57 (\pm 0.03) | 0.51 | 0.58 | 0.61 |
| Cluster means (μ_k): | | | | | | | | |
| Grantham's distance | 63.4 (\pm 3.09) | 57.8 | 63.1 | 68.7 | 82.4 (\pm 3.61) | 76.3 | 82.4 | 88.3 |
| Sneath index | 19.7 (\pm 0.76) | 18.4 | 19.7 | 20.9 | 24.6 (\pm 0.70) | 23.5 | 24.6 | 25.7 |
| SIFT score | 0.38 (\pm 0.04) | 0.33 | 0.38 | 0.43 | 0.03 (\pm 0.03) | 0.02 | 0.03 | 0.03 |
| Polyphen-2 | 0.22 (\pm 0.05) | 0.17 | 0.21 | 0.26 | 0.77 (\pm 0.05) | 0.73 | 0.78 | 0.82 |
| CADD | 15.0 (\pm 0.96) | 13.7 | 14.9 | 16.1 | 24.4 (\pm 0.76) | 24.0 | 24.4 | 24.8 |
| REVEL score | 0.39 (\pm 0.03) | 0.37 | 0.39 | 0.41 | 0.75 (\pm 0.03) | 0.72 | 0.75 | 0.77 |
| MetaLR | 0.81 (\pm 0.01) | 0.80 | 0.81 | 0.83 | 0.95 (\pm 0.01) | 0.94 | 0.95 | 0.95 |
| MutationAssessor | 0.40 (\pm 0.04) | 0.37 | 0.40 | 0.44 | 0.77 (\pm 0.03) | 0.75 | 0.78 | 0.80 |
| Reduced/parsimonious model | | | | | | | | |
| Cluster weights (ω_k): | 0.35 (\pm 0.04) | 0.28 | 0.35 | 0.43 | 0.65 (\pm 0.04) | 0.57 | 0.65 | 0.72 |
| Cluster means (μ_k): | | | | | | | | |
| CADD | 13.2 (\pm 0.89) | 11.5 | 13.2 | 14.9 | 24.2 (\pm 0.26) | 23.7 | 24.2 | 24.6 |
| REVEL score | 0.35 (\pm 0.01) | 0.33 | 0.35 | 0.37 | 0.73 (\pm 0.02) | 0.69 | 0.73 | 0.77 |
| MutationAssessor | 0.36 (\pm 0.03) | 0.30 | 0.36 | 0.41 | 0.76 (\pm 0.02) | 0.72 | 0.76 | 0.78 |

Table 2. Cluster centroid estimates obtained by BGMM using data of the 415 VUS variants.

had a validation accuracy of 89%, a sensitivity of 88%, a specificity of 89%, a positive predictive value (PPV) of 90%, and a negative predictive value (NPV) of 88%. The AUC was 0.93 (95% CI 0.87–0.98). On the test set, the full model achieved an accuracy of 93%, a specificity of 93%, a sensitivity of 92%, a PPV of 91%, and an NPV of 94% (Table 3). The clustering of unlabeled data using the full model presented in Fig. 1.

Deviance information criterion (DIC)-based backward elimination reduced the model dimensionality to a three-parameter mixture model containing only the scores CADD, REVEL, and MutationAssessor. The reduced model had a similar performance and even outperformed the full model for some matrices (Table 4). The models' centroid estimates, predicted labels, and performance metrics were invariant to the seed and priors used.

Upon cluster centroid of SIFT, PolyPhen-2, CADD, REVEL, MetaLR, and MutationAssessor of the full model (Table 2), we developed an Excel-based pathogenicity prediction tool that we called "SanfilippoPred". "SanfilippoPred" considers 2.50%, 50.0%, and 97.5% percentiles for SIFT, PolyPhen, CADD, REVEL, MetaLR, and MutationAssessor. Supplementary (1) shows a brief user guide to how SanfilippoPred works and its requirements.

| | Validation set (n = 99) | | Test set (n = 98) | |
|---------------------|-------------------------|--------|-------------------|--------|
| | Reference | | Reference | |
| | Pathogenic | Benign | Pathogenic | Benign |
| Predicted class | | | | |
| Pathogenic | 45 | 5 | 42 | 4 |
| Benign | 6 | 43 | 3 | 49 |
| Metric | | | | |
| Accuracy (95% CI) | 0.89 (0.81–0.94) | | 0.93 (0.86–0.97) | |
| Balanced accuracy | 0.89 | | 0.93 | |
| No-information rate | 0.52 | | 0.94 | |
| $P_{acc > NIR}$ | < 0.0001 | | < 0.0001 | |
| Sensitivity | 0.88 | | 0.93 | |
| Specificity | 0.89 | | 0.92 | |
| PPV | 0.90 | | 0.91 | |
| NPV | 0.88 | | 0.94 | |
| Cohen's Kappa | 0.78 | | 0.86 | |
| F_1 score | 0.89 | | 0.92 | |

Table 3. Full model confusion matrices and performance measures in the validation and test sets (DIC: 66897.27). DIC, deviance information criterion; NPV, negative predictive value; PPV, positive predicted value.



Figure 1. Correlation and scatterplot matrix between scores for each cluster.

SanfilippoPred outperforms existing genome-wide tools for the classification of known labelling NAGLU, GNS, HGSNAT and SGSH variants

Using the labelled variants of *NAGLU*, *GNS*, *HGSNAT*, and *SGSH* variants ($n = 331$), “SanfilippoPred” performance was compared to the individual genome-wide variant pathogenicity predictors REVEL, CADD, SIFT, Polyphen-2, MutationAssessor, and AlphMissense. “SanfilippoPred” demonstrated superior performance in pathogenicity prediction with an AUC of 0.908 (Fig. 2) and a pathogenicity probability threshold of ≥ 0.50 .

The clinical decision specificity of “SanfilippoPred” showed relative specificity towards known labelling MPS III-relevant variants

To test the clinical decision specificity of MPS III using “SanfilippoPred”, we collected three additional labelled missense variant sets as an independent specificity test datasets. This dataset included 96 known pathogenicity variants for the *Nkx2-5*, *GATA4*, and *Cox10* genes that were registered in the Ensembl database with the criteria provided. The overall matrices of sensitivity, specificity, accuracy, and precision showed the relative specificity of our tool to MPS III-relevant variants, as shown in Fig. 3 and Table 5.

To identify the sensitivity threshold of the SanfilippoPred tool, we used high-confidence pathogenic and likely-pathogenic *NAGLU* variants from the ClinVar database. Pathogenicity prediction probabilities of

| Predicted class | Validation set (n=99) | | Test set (n=98) | |
|---------------------|-----------------------|--------|------------------|--------|
| | Reference | | Reference | |
| | Pathogenic | Benign | Pathogenic | Benign |
| Pathogenic | 46 | 7 | 46 | 8 |
| Benign | 3 | 43 | 1 | 43 |
| Metric | | | | |
| Accuracy (95% CI) | 0.90 (0.82–0.95) | | 0.91 (0.83–0.96) | |
| Balanced accuracy | 0.90 | | 0.91 | |
| No-information rate | 0.51 | | 0.52 | |
| $P_{acc > NIR}$ | < .0001 | | < .0001 | |
| Sensitivity | 0.94 | | 0.98 | |
| Specificity | 0.86 | | 0.84 | |
| PPV | 0.87 | | 0.85 | |
| NPV | 0.94 | | 0.98 | |
| Cohen's Kappa | 0.80 | | 0.82 | |
| F_1 score | 0.91 | | 0.91 | |

Table 4. Parsimonious model confusion matrices and performance measures in the validation and test sets (DIC: 13545.79).

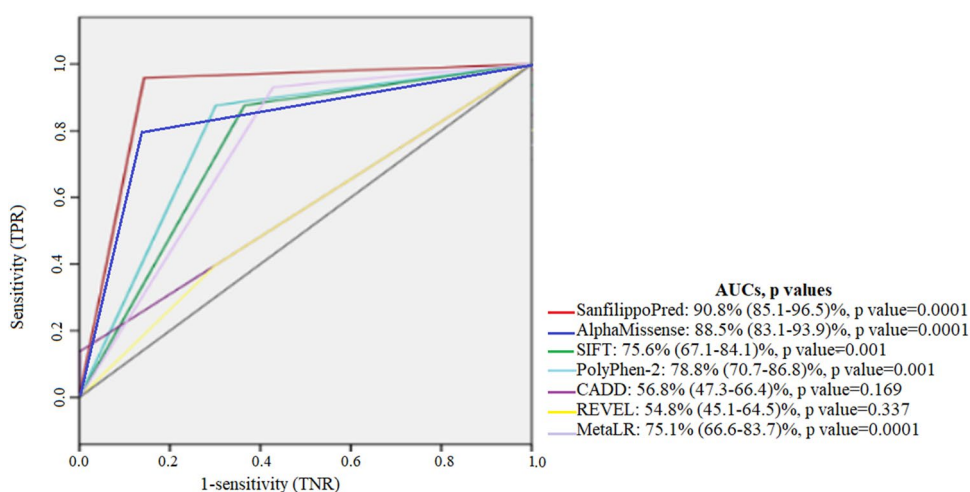


Figure 2. Comparison of receiver operating characteristic (ROC) curves of existing prediction scores and SanfilippoPred scores using all labelled missense variants of NAGLU, GNS, HGSNAT, and SGSH genes (n = 331). The AUCs showed that SanfilippoPred maximizes the identification of both pathogenic and benign variants in those genes.

“SanfilippoPred” were highly concordant with consensus ClinVar classifications demonstrating 0.857 sensitivity. Therefore, 0.857 is considered a sensitivity threshold of the SanfilippoPred calculator tool.

Discussion

The prevalence of increasingly large numbers of genetic variations led to the necessity of predictor and prioritize variant tools, especially since the vast majority of these variants are defined as variants of uncertain significance (VUS)^{14,15}. Accurate pathogenicity prediction of missense variants is essential in genetic studies, clinical diagnosis, healthcare support, and clinical decision-making. Most approaches to predicting the functional effects or pathogenicity of missense variations rely on either sequence or structural information. However, machine learning is a new model to predict the pathogenicity of missense variants in the human genome¹⁶.

Our “SanfilippoPred” groups together the four genes associated with MPS III. These variants are missense with criteria provided and extracted from Ensembl 108, and they are clinically asserted from ClinVar, LOVD, VARCARDS, and ACMG (Franklin, Geenox) databases to avoid biased annotation in the individual database.

Based on our hypothesis that the MPS III-relevant variant pathogenicity prediction tools may be improved by using gene and disease-specific datasets supplemented with complementary multi-scale computational tools, we used a Bayesian Gaussian mixture model to explore the hidden relationships among eight computational scores

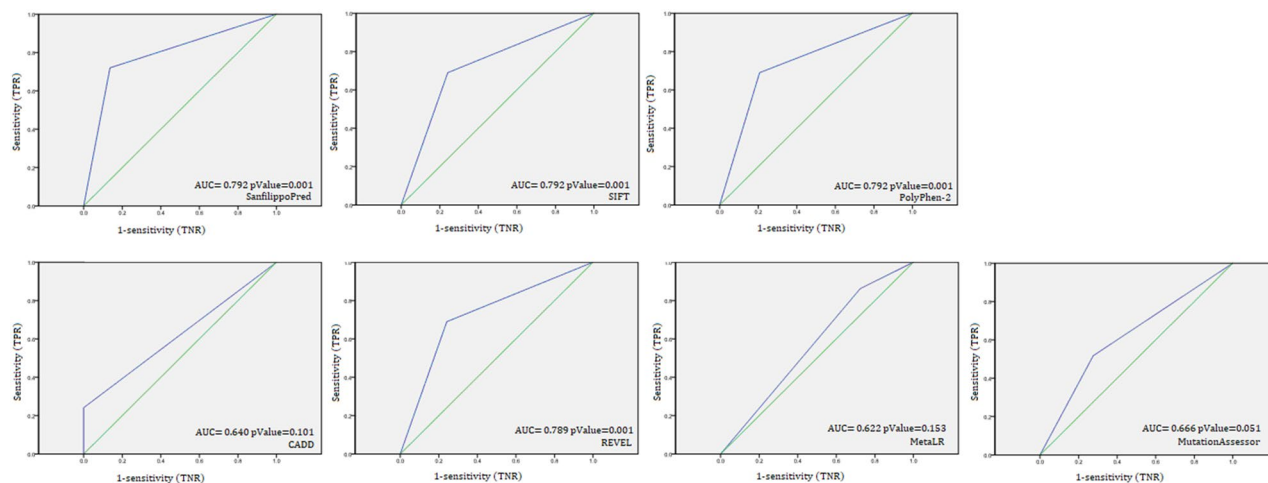


Figure 3. Receiver operating characteristic (ROC) curves of existing prediction scores and SanfilippoPred scores using all labelled missense variants of the *Nkx2-5*, *GATA4*, and *COX10* genes. The AUCs showed that SanfilippoPred has powerful discrimination towards Sanfilippo-relevant variants.

| ROC matrices | SanfilippoPred | SIFT | PolyPhen-2 | CADD | REVEL | MetaLR | variantAssessor |
|--------------|----------------|-------|------------|-------|-------|--------|-----------------|
| Sensitivity | 0.720 | 0.690 | 0.690 | 0.241 | 0.690 | 0.862 | 0.517 |
| Specificity | 0.864 | 0.759 | 0.793 | 1 | 0.759 | 0.276 | 0.724 |
| Accuracy | 0.787 | 0.724 | 0.741 | 0.621 | 0.724 | 0.569 | 0.621 |
| Precision | 0.857 | 0.741 | 0.769 | 1 | 0.741 | 0.543 | 0.652 |

Table 5. Performance of SanfilippoPred tool against number of the wide-genome prediction tools.

for VUS missense variants of the *NAGLU* gene, using the score values as features in the training dataset. We developed “SanfilippoPred” to avoid the pitfalls of relying on genome-wide variant classifiers in variant pathogenicity interpretation and to support the clinical decision of MPS III over the currently available genome-wide tools. Validation and test datasets showed high sensitivity and specificity. Moreover, to predict the pathogenicity of *NAGLU* VUS variants, in addition, “SanfilippoPred” showed a powerful tool for true pathogenic *NAGLU* variants with 85.7% sensitivity.

Supporting our hypothesis regarding disease-specific predictors is Zhang et al.¹¹ disease-specific variant classifier, “CardioBoost”, which has high global discrimination accuracy (precision recall area under the curve [AUC] = 0.91 for cardiomyopathies and 0.96 for arrhythmias¹¹). Similarly, Hutter et al.¹⁷ developed “HePPy” (Haematological Predictor of Pathogenicity) with impressive discrimination performance for somatic disease-causing variants in a haematological setting¹⁷. Furthermore, regarding gene-specific predictors as reported by Li et al.¹⁴, their predictor tool called “vERnet-B” accurately predicts BRCA1 pathogenicity recognition through its tertiary structure features derived from the “AlphaFold2” tool¹⁴.

It is well known that the advantages of disease-specific training datasets are; (1) decreasing the false prediction of benign variants as disease-causing, and (2) establishing the relationship between pathogenicity impact and gene nature. It is worth noting that every group of genes has distinct molecular mechanisms and biological functions. Zhang et al.¹¹ pointed that disease pathogenicity-specific tools are most powerful in the genotype–phenotype relationship, and overcome the false negative pathogenicity rate of genome-wide tools because they are trained on universal labels¹¹.

Defect in one of the four genes; *NAGLU*, *GNS*, *HGSNAT*, and *SGSH* is causing four subtypes of MPS III. It is worth noting that we observed (1) consistent sensitivity, specificity, accuracy, and precision scores of SanfilippoPred, and (2) relative performance convergence between our tool and SIFT and PolyPhen-2 tools, as shown in Fig. 4. The consistent scores of the SanfilippoPred tool may reflect its interpretation stability and external validity. Also, the convergence manner between our SanfilippoPred, SIFT, and PolyPhen-2 tools may refer to amino acid conservation and physicochemical properties distances, whose effect on the protein structure could play a significant role in the pathogenicity of MPS III variants. Interestingly, Clark et al.¹⁸ pointed out that sequence conservation is important to predict the impact of missense variants on the enzymatic activity of *NAGLU*¹⁸.

Conclusions

Our study had some limitations that are; (1) we have considered the prediction of pathogenicity for only the missense variants, and other variant classes may consider low-confidence training data, (2) all included gene variants associated with MPS III subtypes only, (3) some pathogenicity evidence was neglected during SanfilippoPred modelling, such as minor allele frequency, (4) the SanfilippoPred calculator tool has constrain

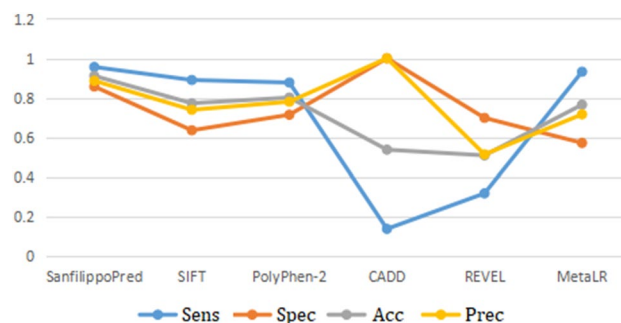


Figure 4. Receiver operating characteristic (ROC) curve matrices of our SanfilippoPred calculator tool and five individual predictors showing (1) consistent sensitivity, specificity, accuracy, and precision scores of the SanfilippoPred calculator tool, (2) relative performance convergence among SanfilippoPred and both SIFT and PolyPhen-2, and (3) outperforming the SanfilippoPred tool over five genome-wide tools.

limits, such as indeterminate feature scores, and (5) we intended to adopt an unsupervised machine learning approach, so any different learning framework structure may give different output. “SanfilippoPred” is mainly developed to predict the pathogenicity of MPS III variants, not as a standalone clinical decision tool.

Finally, “SanfilippoPred” confirmed the hypothesis that a single pathogenic score cannot capture the true pathogenicity of a variant decision, and gene-disease-specific pathogenicity tools are recommended.

Methods

Missense variants extraction and training dataset

A total of 612 missense variants of the N-acetyl-alpha-glucosaminidase (*NAGLU*) gene were extracted from Ensembl 108 (accessed in April 2021). All variants with controversial clinical significance and those associated with other diseases other than MPS III were excluded. All MPS III-relevant missense variants were asserted according to the status of reviewing as “criteria provided” from the submitter or “reviewed by expert panel” in the ClinVar, Ensembl, LOVD, VARCARDS (damage score equal to one for pathogenic, less than or equal to 0.3 for benign) and ACMG (Franklin, Genoox) databases. The asserted missense variants were categorized in two groups according to their clinical significance; (1) unlabelled variants that include 415 variants (67.8%) with VUS assertion, (2) labelled variants that include 101 variants (16.5%) with benign or likely benign assertion, and 96 variants (15.7%) with pathogenic or likely pathogenic assertion.

All 415 unlabelled missense variants formed the training dataset. All variants of the training dataset had known values of the pathogenicity prediction scores Polyphen-2, SIFT, REVEL, CADD, MetaLR, and MutationAssessor, in addition to Sneath’s and Grantham’s scores as conservation predictors. Parameters of extraction and clinical assertion are shown in Table 6.

Modeling

The analysis and modeling were performed using R software (version 4.1.1). Missing values in the training, validation and test datasets were imputed using the “MICE” package (version 3.13.0). The imputation method used was predictive mean matching (PMM).

Concerning the unlabeled variant data, a Bayesian Gaussian Mixture Model (BGMM) was fitted to cluster the data and obtain parameter estimates for each cluster with 95% credible intervals. The model was set to predict

| Extraction resources | ensembl (Ensembl Release 108) |
|-----------------------------------|---|
| Clinical pathogenicity resources | ClinVar |
| | LOVD v. 3.0 |
| | VARCARDS |
| | ACMG (Franklin, Genoox) |
| HGNC Symbol/ID | NAGLU/7632 |
| Location | Ch17: 42,536,241-42,544,449 |
| Transcript | ENST00000225927.7 NAGLU-201 (NM_000263.4) |
| Transcripts flag | MANE only |
| consequences | Missense |
| Clin. significance | VUS, benign, likely benign, pathogenic, likely pathogenic |
| Selected pathogenicity predictors | Polyphen-2, SIFT, REVEL, CADD, MetaLR, MutationAssessor, Sneath’s and Grantham’s scores |

Table 6. parameters of extraction and clinical assertion of *NAGLU* missense variants (n = 612).

the probability of whether the variant belongs to one of the two clusters, whether the variant of interest is likely benign, or truly benign or likely pathogenic or truly pathogenic.

Priors

A Gibbs sampler was manually coded to sample from the posterior distribution using conjugate priors on cluster weights, mean vectors, and covariance matrices; the prior inferred on cluster weights was a Dirichlet prior in the form $\omega_k \sim \text{Dir}(1, 1)$ for $k \in \{1, 2\}$, a multivariate normal prior on cluster means in the form of $\mu_k \sim \mathcal{N}(\eta, \tau)$, where η is the prior mean vector, which was taken as the mean vector of the observed data, and τ is the prior covariance and was taken as the covariance matrix of the observed data, scaled by a factor of 10, and an inverse Wishart prior on covariance matrices in the form of $\Sigma_k \sim W_p^{-1}(v, \Psi)$, where v is the prior degrees of freedom and Ψ is a $p \times p$ positive definite scale matrix, p is the number of parameters in the model, and the prior value of v was taken as p and Ψ as the covariance matrix of the whole data.

To resolve the problem of label switching, a constraint was set on the cluster weights, such that $\omega_1 < \omega_2$, assuming that ω_1 is the cluster weight for benign variants and ω_2 for pathogenic variants (in other words, we assumed a priori that the probability that a variant is benign is less than the probability that it is pathogenic). Then, the MCMC output was reordered based on the weight constraint.

Backward elimination using the deviance information criterion (DIC) was performed to identify a parsimonious model. Both the full and parsimonious models were validated and tested on labelled data, and confusion matrix statistics (including accuracy, sensitivity, specificity, positive, and negative predictive values) were reported for each model. Validation and test data were partitioned equally, with an equal probability of sampling benign and pathogenic variants in each set.

Predictions were made based on the posterior predictive distribution using the following formula:

$$p_{i,k,m} = \frac{\omega_{k,m} |2\pi \sum_{k,m} |^{-\frac{1}{2}} e^{-\frac{1}{2}} (x_i - \mu_{k,m})^T \sum_{k,m}^{-1} (x_i - \mu_{k,m})}{\sum_{k=1}^K \omega_{k,m} |2\pi \sum_{k,m} |^{-\frac{1}{2}} e^{-\frac{1}{2}} (x_i - \mu_{k,m})^T \sum_{k,m}^{-1} (x_i - \mu_{k,m})}$$

where $p_{i,k,m}$ is the probability that observation i belongs to cluster k for the Monte-Carlo sample m . For each m , the classification $\hat{c}_{i,m}$ was obtained by $\arg\max_k \in \{1, 2\} (p_{i,k,m})$, and the final classification \hat{c}_i was made by taking the mode of $\hat{c}_{i,m}$.

Model performance evaluation

The model was tested on the test and validation datasets, and the area under the curve (AUC), sensitivity, specificity, accuracy, precision, positive predictive value (PPV), negative predictive value (NPV), no-information rate (NIR), Cohen's kappa, and the F1 score were calculated. Accuracy and NIR were compared using the exact binomial test (implemented by the caret package in R) calculated based on the results of receiver operating characteristic (ROC) curves. AUC measures the whole probability power of our ML predictor, sensitivity measures the true positive (pathogenic variants) rate by $\text{Sens.} = \text{TP}/(\text{TP} + \text{FN})$, specificity measures the true negative (benign variants) rate by $\text{Spec} = \text{TN}/(\text{TN} + \text{FP})$, accuracy measures the number of correct predictions, either positive or negative, by $\text{Acc.} = (\text{TN} + \text{TP})/(\text{TN} + \text{TP} + \text{FN} + \text{FP})$, and precision measures rate of true positive belong to all positive predictions by $\text{Prec.} = \text{TP}/(\text{TP} + \text{FP})$.

To further evaluate our model, we extracted missense variants of the *GNS*, *HGSNAT* and *SGSH* genes using the same extraction parameters as the *NAGLU* gene variants. Then, we used our model to predict the pathogenicity of their variants, and the corresponding ROC curves were analysed.

Genome-wide prediction tools for comparison

We compared the ROC curve data of our ML predictor for all extracted *NAGLU*, *GNS*, *HGSNAT*, and *SGSH* variants against individual REVEL, CADD, SIFT, Polyphen-2, MutationAssessor, and AlphMissense data for the same variants. Area under the curve (AUC), sensitivity, specificity, accuracy, and precision were measured.

96 known labelled variants for the *Nkx2-5*, *GATA4*, and *Cox10* genes (registered in the Ensembl database with criteria) were extracted to test the clinical decision specificity of our ML model towards MPS III-relevant genes against non-MPS III-relevant ones.

Evaluation of "SanfilippoPred" sensitivity

In June 2021, we accessed the ClinVar dataset and extracted pathogenic and likely pathogenic *NAGLU* variants with a two-star review status (i.e., criteria provided, multiple submitters, and no conflicts found). Twenty-one missense variants were collected to test the sensitivity threshold of "SanfilippoPred".

Data availability

The datasets used and/or analysed during the current study are available from the corresponding author upon reasonable request.

Received: 26 October 2023; Accepted: 16 May 2024

Published online: 27 May 2024

References

1. Neufeld, E. F. & Muenzer, J. The mucopolysaccharidoses. In *The Metabolic and Molecular Bases of Inherited Disease* (eds Scriver, C. R. et al.) 3421–3452 (McGraw-Hill, 2001).

2. Sanfilippo, S. J., Podosin, R. L., Langer, L. O. & Good, R. A. Mental retardation associated with acid mucopolysacchariduria (heparitin sulfate type). *J. Pediatr.* **63**, 837–838 (1963).
3. Andrade, F., Aldámiz-Echevarría, L., Llaena, M. & Couce, M. L. Sanfilippo syndrome: Overall review. *Pediatr. Int.* **57**, 331–338. <https://doi.org/10.1111/ped.12636> (2015).
4. De Pasquale, V. & Pavone, L. M. Heparan sulfate proteoglycans: The sweet side of development turns sour in mucopolysaccharidoses. *Biochim. Biophys. Acta Mol. Basis Dis.* **1865**, 165539. <https://doi.org/10.1016/j.bbadis.2019.165539> (2019).
5. Birrane, G. *et al.* Structural characterization of the α -N-acetylglucosaminidase, a key enzyme in the pathogenesis of Sanfilippo syndrome B. *J. Struct. Biol.* **205**, 65–71. <https://doi.org/10.1016/j.jsb.2019.02.005> (2019).
6. Whiteman, P. & Henderson, H. A method for the determination of amniotic-fluid glycosaminoglycans and its application to the prenatal diagnosis of Hurler and Sanfilippo diseases. *Clin. Chim. Acta* **79**, 99–105 (1977).
7. Marsh, J. & Fensom, A. H. 4-Methylumbelliferyl α -N-acetylglucosaminidase activity for diagnosis of Sanfilippo B disease. *Clin. Genet.* **27**, 258–262 (1985).
8. Peterson, T. A., Doughty, E. & Kann, M. G. Towards precision medicine: Advances in computational approaches for the analysis of human variants. *J. Mol. Biol.* **425**, 4047–4063. <https://doi.org/10.1016/j.jmb.2013.08.008> (2013).
9. Ioannidis, N. M. *et al.* REVEL: An ensemble method for predicting the pathogenicity of rare missense variants. *Am. J. Hum. Genet.* **99**, 877–888. <https://doi.org/10.1016/j.ajhg.2016.08.016> (2016).
10. Li, Q. *et al.* Gene-specific function prediction for non-synonymous variants in monogenic diabetes genes. *PLoS ONE* **9**, e104452. <https://doi.org/10.1371/journal.pone.0104452> (2014).
11. Zhang, X. *et al.* Disease-specific variant pathogenicity prediction significantly improves variant interpretation in inherited cardiac conditions. *Genet. Med.* **23**, 69–79. <https://doi.org/10.1038/s41436-020-00972-3> (2021).
12. Ruklisa, D., Ware, J. S., Walsh, R., Balding, D. J. & Cook, S. A. Bayesian models for syndrome- and gene-specific probabilities of novel variant pathogenicity. *Genome Med.* **7**, 5. <https://doi.org/10.1186/s13073-014-0120-4> (2015).
13. Richards, S. *et al.* Standards and guidelines for the interpretation of sequence variants: A joint consensus recommendation of the American College of Medical Genetics and Genomics and the Association for Molecular Pathology. *Genet. Med.* **17**, 405–424. <https://doi.org/10.1038/gim.2015.30> (2015).
14. Li, C. *et al.* Artificial intelligence-based recognition for variant pathogenicity of BRCA1 using AlphaFold2-predicted structures. *Theranostics* **13**, 391–402. <https://doi.org/10.7150/thno.79362> (2023).
15. McCoy, M., Hamre, J., Klimov, D. K. & Saleet Jafri, M. Predicting genetic variation severity using machine learning to interpret molecular simulations. *Biophys. J.* **120**, 189–204. <https://doi.org/10.1016/j.bpj.2020.12.002> (2021).
16. Pejaver, V., Mooney, S. D. & Radivojac, P. Missense variant pathogenicity predictors generalize well across a range of function-specific prediction challenges. *Hum. Mutat.* **38**, 1092–1108. <https://doi.org/10.1002/humu.23258> (2017).
17. Hutter, S. *et al.* A novel machine learning based in silico pathogenicity predictor for missense variants in a hematological setting. *Blood J.* **134**(1), 2090 (2019).
18. Clark, W. T. *et al.* Assessment of predicted enzymatic activity of α -N-acetylglucosaminidase variants of unknown significance for CAGI 2016. *Hum. Mutat.* **40**, 1519. <https://doi.org/10.1002/humu.23875> (2019).

Author contributions

Eman E.A. Mohammed and Alaaeldin G. Fayez contributed to the study's conception and design. Eman E.A. Mohammed contributed to variant dataset extraction and its annotations under the supervision of Alaaeldin G. Fayez. Nabil M. Abdelfattah performed the machine learning modelling. Alaaeldin G. Fayez measured the performance of the SanfilippoPred tool using ROC analysis and constructed a SanfilippoPred tool. Alaaeldin G. Fayez and Eman E.A. Mohammed were major contributors to writing the manuscript. Ekram M. Fateen revised the manuscript. All authors read and approved the final manuscript.

Funding

Open access funding provided by The Science, Technology & Innovation Funding Authority (STDF) in cooperation with The Egyptian Knowledge Bank (EKB).

Competing interests

The authors declare no competing interests.

Additional information

Supplementary Information The online version contains supplementary material available at <https://doi.org/10.1038/s41598-024-62352-0>.

Correspondence and requests for materials should be addressed to E.E.A.M.

Reprints and permissions information is available at www.nature.com/reprints.

Publisher's note Springer Nature remains neutral with regard to jurisdictional claims in published maps and institutional affiliations.



Open Access This article is licensed under a Creative Commons Attribution 4.0 International License, which permits use, sharing, adaptation, distribution and reproduction in any medium or format, as long as you give appropriate credit to the original author(s) and the source, provide a link to the Creative Commons licence, and indicate if changes were made. The images or other third party material in this article are included in the article's Creative Commons licence, unless indicated otherwise in a credit line to the material. If material is not included in the article's Creative Commons licence and your intended use is not permitted by statutory regulation or exceeds the permitted use, you will need to obtain permission directly from the copyright holder. To view a copy of this licence, visit <http://creativecommons.org/licenses/by/4.0/>.

© The Author(s) 2024